Journal of Nonlinear and Convex Analysis
Volume 26, Number 6, 2025, 1909–1920

Yokohama Publishers
ISSN 1880-5221 ONLINE JOURNAL

BEARING FAULT DIAGNOSIS OF WIND TURBINE BASED ON INSTANTANEOUS INFORMATION OF INTRINSIC TIME-SCALE DECOMPOSITION

XUELI AN*, TINGWEI WU, ZHUANG FU, AND YINGYU LU

Abstract. The vibration patterns from wind turbine bearing issues are exceedingly intricate. A novel approach for diagnosing these bearing faults in wind turbines has been developed, leveraging the instantaneous data from intrinsic time-scale decomposition. This method demonstrates a marked enhancement in computational efficiency and precision compared to empirical mode decomposition and local mean decomposition. Initially, the bearing's acceleration vibration signal is dissected into multiple suitable rotational components.Then the frequency domain analyses of the instantaneous amplitude and instantaneous phase of rotation components containing obvious impact components are made to abstract the features of bearing faults. Finally, the vectors of fault features are input neural network to identify wind turbine bearing faults. The findings suggest that the suggested approach can effectively identify wind turbine bearing issues with a high degree of precision and computational speed.

1. Introduction

As the largest development potential new and renewable energy, wind energy developed at a remarkable pace in recent years. According to the Global Wind Energy Council, the worldwide installed wind power capacity reached 1021 GW by the end of 2023, with China accounting for 441 GW of that total, is the most country of installed capacity [7]. Since wind turbines' operating environment is harsher, with the increase of their total running time, their parts are prone to malfunction [4–6,11]. In the faults of wind turbine, bearing faults constitute a significant proportion [2], the faults' vibration signal is very complex. The maintenance cost of a large wind farm accounts for 15% to 35% of the revenue of the wind farm. Therefore, it is necessary to carry out timely health monitoring to reduce maintenance costs. Research shows that the rotor hub and transmission components of wind turbines nearing their end of life are more prone to catastrophic failures, and the long-term unplanned maintenance downtime caused by such components accounts for 30% to 60% of the total operating and maintenance costs of wind turbines.

2020 *Mathematics Subject Classification.* 60G35, 94A12.

Key words and phrases. Wind turbine, spherical roller bearing, intrinsic time-scale decomposition, instantaneous amplitude, instantaneous phase, fault diagnosis.

This work was supported by the IWHR Research & Development Support Program (TJ0145B022021).

*Corresponding author.

Time-frequency analysis methods are commonly used techniques for handling with nonlinear and nonstationary signals. For example, Empirical mode decomposition (EMD) and local mean decomposition (LMD) are techniques that can effectively uncover the constituents of a signal across both temporal and spectral dimensions, and have been extensively adapted to mechanical fault diagnosis. although EMD has undergone significant development, it still has problems such as end point effect, mode mixing and negative frequency. Compared with EMD, LMD has achieved more significant improvements not only in the terminal effect but also negative frequency. However, the calculation speed is slower, and there are also false components. Intrinsic time-scale decomposition (ITD), introduced by Frei and Osorio, can break down intricate, nonstationary, and nonlinear signals into multiple appropriate rotational components, effectively capturing the dynamic traits of these fluctuating signals. This method boasts a superior computational efficiency, frequency resolution and dismantling efficiency for the real-time processing of nonstationary signals with time-varying characteristics. Wang [9] used the ITD method to adaptively decompose the switch machine pressure signal into a range of intrinsic rotational components, which effectively represented the different local features of the pressure signal. Yu [10] utilized the ITD method's adaptive decomposition ability for signals, thereby improving the accuracy of signal output.

The ITD method has not interpolation and selection process, Thus, the immediate amplitude and phase obtained can instantly mirror the time-frequency characteristics of the original signal.

This paper introduces a fault diagnosis technique for wind turbine bearings utilizing ITD instantaneous data. Initially, ITD is utilized to effectively break down the intricate vibration acceleration signals from wind turbine bearing faults into several suitable rotational components.Afterwards, the proper rotation components (PRCs) with containing significant periodic impact composition are found, the PRCs' instantaneous amplitude and instantaneous phase are analyzed in frequency domain to obtained feature vectors of bearing faults. Finally, the feature vectors input to the neural network to identify wind turbine bearing faults.

This paper elaborates on the mathematical principles of the ITD method in Section 2, and outlines the procedure for identifying faults in wind turbine bearings using the intrinsic time scale decomposition of immediate data in Section 3. In Section 4, the approach is demonstrated to be highly effective for diagnosing faults in real-world wind turbines. The section 5 concludes with a summary.

2. Intrinsic time-scale decomposition method

ITD [3,8] method's computing speed is more superior than EMD and LMD. Complex vibration signal can be decomposed into independent PRCs and a convergent component. The detail introduction of ITD method as follows:

The definitions of signal X_t, ξ are reference elements which extract a reference signal from the signal X_t, leaving a residual signal called proper rotation. A decomposition of X_t as follows:

$$X_t = \xi X_t + (1-\xi)X_t = L_t + H_t \tag{2.1}$$

where $L_t = \xi X_t$ is baseline signal, $H_t = (1-\xi)X_t$ is proper rotation component.

(1) The local extrema $\{\tau_k, k = 1, 2, \ldots, n\}$ of a signal X_t is determined, where $\tau_0 = 0$. The $X(\tau_k)$ and $L(\tau_k)$ are abbreviated as X_k and L_k, assuming L_t and H_t are defined in $[0, \tau_k]$, and X_t is available for $t \in [0, \tau_{k+2}]$.

(2) The baseline-extracting factor ξ in interval $(\tau_k, \tau_{k+1}]$ between consecutive extrema is defined as:

$$\xi X_t = L_t = L_k + \left(\frac{L_{k+1} - L_k}{X_{k+1} - X_k}\right)(X_t - X_k) \tag{2.2}$$

where

$$L_{k+1} = \alpha\left[X_k + \left(\frac{\tau_{k+1} - \tau_k}{\tau_{k+2} - \tau_k}\right)(X_{k+2} - X_k)\right] + (1 - \alpha)X_{k+1} \tag{2.3}$$

where $\alpha \in (0, 1)$, it is generally fixed with 0.5.

(3) The ψ is defined as proper rotation extraction operator, then $H_t^1 = \psi X_t = X_t - \xi X_t = X_t - L_t^1$ is proper rotation component (PRC) which has the highest relative frequency. The highest relative frequency is the value corresponding to the frequency component with the largest frequency value in a signal decomposition. The baseline signal L_t^1 as the input signal, repeat these steps until the baseline signal is monotonic. The entire decomposition process can be represented as:

$$\begin{aligned} X_t = \psi X_t + \xi X_t &= \psi X_t + (\psi + \xi)\xi X_t \\ &= [\psi(1 + \xi) + \xi^2]X_t \\ &= \left(\psi \sum_{k=0}^{p-1} \xi^k + \xi^p\right) X_t \end{aligned} \tag{2.4}$$

where $\psi\xi^k X_t$ is the $(k + 1)$st level proper rotation, $\xi^p X_t$ is the monotonic trend. The ITD approach introduced a novel concept for instantaneous amplitude, phase, and frequency, with the instantaneous phase θ_t being characterized as:

$$\theta_t = \begin{cases} \left(\dfrac{x_t}{A_1}\right)\dfrac{\pi}{2}, & t \in [t_1, t_2), \\ \left(\dfrac{x_t}{A_1}\right)\dfrac{\pi}{2} + \left(1 - \dfrac{x_t}{A_1}\right)\pi, & t \in [t_2, t_3), \\ \left(-\dfrac{x_t}{A_2}\right)\dfrac{3\pi}{2} + \left(1 + \dfrac{x_t}{A_2}\right)\pi, & t \in [t_3, t_4), \\ \left(-\dfrac{x_t}{A_2}\right)\dfrac{3\pi}{2} + \left(1 + \dfrac{x_t}{A_2}\right)2\pi, & t \in [t_4, t_5) \end{cases} \tag{2.5}$$

where $A_1 > 0, A_2 > 0$, they respectively denote a full-wave's amplitude of positive half-waves and negative half-waves. t_1 and t_5 are the time of two successive zero up-crossings. t_2 marks the moment when the positive half-wave reaches its peak (A1). t_3 indicates the instant when the waveform crosses zero while descending. t_4 signifies the time at which the negative half-wave hits its lowest point (-A2). The full-wave refers to the segment of the signal from one zero up-crossing to the next. The half-wave is defined as the part of the signal that spans between two consecutive zero crossings. A monotone interval is the section of the signal that lies between two neighboring extreme points.

The instantaneous frequency f_t can be derived from the instantaneous phase θ_t through differentiation, as shown below:

$$f_t = \frac{1}{2\pi}\frac{d\theta_t}{dt}. \tag{2.6}$$

The instantaneous amplitude A_t is defined based on half-wave, A_t is calculated based on the peak values of the correct rotations occurring between zero points, as outlined below:

$$A_t = \begin{cases} A_1, & t \in [t_1, t_3), \\ -A_2, & t \in [t_3, t_5). \end{cases}. \tag{2.7}$$

The ITD technique successfully captures the intrinsic properties of the signal. This approach is particularly well-suited for examining signals that include Amplitude Modulation-Frequency Modulation (AM-FM) elements. Essentially, the ITD method addresses and resolves all the drawbacks associated with EMD. First, the computational complexity of ITD is only O(n), which is much lower than that of EMD. Second, when applied to data windows, the randomness of ITD makes the edge effects generated by the signal in the window not interfere with each other, unlike those generated by EMD. Finally, when EMD tries to perform time-frequency energy analysis, a special filtering process must be referenced, which is not required by ITD, which also leads to higher efficiency of ITD than EMD.

This study employs the ITD algorithm to dissect the vibration signal from wind turbine bearing faults, isolating the key components' instantaneous amplitudes and phases. By examining their frequency spectra, this method can accurately pinpoint the specific fault traits in wind turbine bearings.

3. Fault diagnosis method of wind turbine bearing based on ITD instantaneous information

Due to the influence of wind conditions and the intrinsic properties of roller bearings, when a fault occurs in a wind turbine's roller bearing, the resulting vibration signal typically exhibits a complex modulation pattern. In order to better identify wind turbine bearing fault, it is needed to effectively extract fault features. ITD method has used to effectively decompose vibration acceleration signal to obtain PRCs, $c_1, c_2, \ldots, c_n$. The PRCs which contains obvious periodic impact composition are selected in this paper. Their instantaneous amplitude and instantaneous phase is analyzed in frequency domain using the equations (3.1) $\sim$ (3.4). And bearing fault features $AP_i = [A_i(u_{mf}),\ A_i(u_{fc}),\ A_i(u_{rmsf}),\ A_i(u_{stdf}),\ P_i(u_{mf}),\ P_i(u_{fc}),\ P_i(u_{rmsf}),\ P_i(u_{stdf})]$ are extracted. Where i represents the i-th proper rotation component c_i; $A_i(u_{mf})$, $A_i(u_{fc})$, $A_i(u_{rmsf})$, $A_i(u_{stdf})$, represents instantaneous amplitude's frequency-domain characteristics; $P_i(u_{mf})$, $P_i(u_{fc})$, $P_i(u_{rmsf})$, $P_i(u_{stdf})$, represents instantaneous phase's frequency-domain characteristics.

Frequency mean:

$$u_{mf} = \frac{1}{K}\sum_{k=1}^{K} s(k). \tag{3.1}$$

Frequency center:

$$u_{fc} = \frac{\sum_{k=1}^{K} f_k s(k)}{\sum_{k=1}^{K} s(k)}. \tag{3.2}$$

Frequency root mean square value:

$$u_{rmsf} = \sqrt{\frac{\sum_{k=1}^{K} f_k^2 s(k)}{\sum_{k=1}^{K} s(k)}}. \tag{3.3}$$

Frequency standard deviation:

$$u_{stdf} = \sqrt{\frac{\sum_{k=1}^{K} [f_k - t_{fc}]^2 s(k)}{\sum_{k=1}^{K} s(k)}}. \tag{3.4}$$

In the formula (3.1) $\sim$ (3.4), $s(k)$ is frequency spectrum of vibration signal, where $k = 1, \ldots, K$, and K represents the total number of frequency spectral lines; f_k denotes the frequency value of the k-th line in the spectrum.

When wind turbine's bearing occurs faults, shock signal is generated. This makes the spectrum of instantaneous amplitude and instantaneous phase for PRCs (c_i) will change, and the main spectral energy peak position also changes [12]. Thus, effectively analyze the frequency features of c_i's instantaneous information will well get the unit device's running condition. Since the ITD method can decompose vibration signal into several PRCs whose frequency portion ordered arrangement. And in the high frequency part, the features of the roller bearing are concentrated [1]. Therefore, it is only necessary to analyze the first few PRCs. The vectors AP serve as fault characteristic vectors, and a neural network approach is utilized to detect faults in wind turbine roller bearings.

The methodology for diagnosing wind turbine bearing faults using ITD instantaneous data is illustrated in Figure 1. The detailed steps are as follows:

(1) Under laboratory conditions, main shaft bearing faults of direct-drive wind turbine which occur frequently are simulated. The issues encompass defects in the outer ring, inner ring, and rolling elements. Additionally, a bearing under normal operational conditions is also simulated. Vibration acceleration signals from the bearing in these four scenarios are utilized as both sample and test data. For this study, spherical roller bearings, commonly employed in real-world wind turbines, are chosen for the experiments.

(2) The intrinsic time scale decomposition (ITD) technique is employed to break down the vibration acceleration signal. This process allows both the sample and test data signals to be separated into a sequence of PRCs $(c_1, c_2, \ldots, c_n)$, each representing distinct characteristic scales;

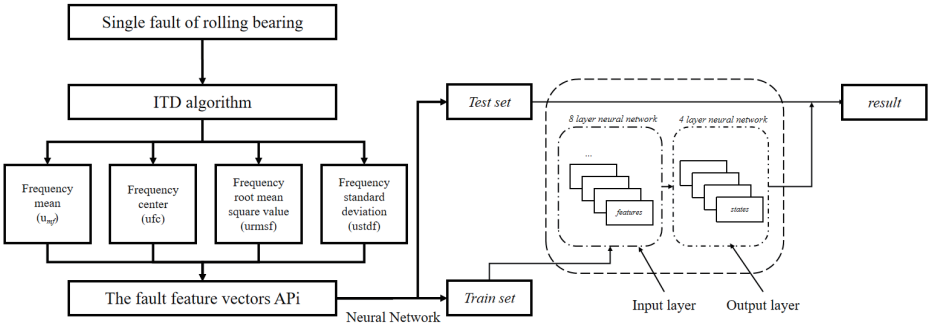

FIGURE 1. Flowchart of Fault Diagnosis Process Based on ITD.

(3) The instantaneous information (instantaneous amplitude and instantaneous phase) of the first k PRCs which contains evident periodic impact components is analyzed in frequency domain, the bearing feature vectors $AP_i = [A_i(u_{mf}), A_i(u_{fc}), A_i(u_{rmsf}), A_i(u_{stdf}), P_i(u_{mf}), P_i(u_{fc}), P_i(u_{rmsf}), P_i(u_{stdf})]$ are extracted, where $i = 1, 2, \ldots, k$;

(4) The fault feature vectors AP_i is input to the neural network for training:

Neural network comprises interconnected nodes, or neurons, which process and transmit information. This technology finds wide-ranging uses in various domains, including visual identification and the processing of human language.

Initially, determining the suitable number of layers, the quantity of neurons per layer, and the activation functions for a neural network is contingent upon the specific characteristics and intricacy of the problem. Through the application of optimization techniques such as gradient descent, the parameters, including weights and biases, are fine-tuned to reduce the loss function, which quantifies the discrepancy between the forecasted and the true outcomes.

(5) Once the training is satisfactory, using the trained neural network to identify the test samples.

4. Experiment validation

4.1. **Experiment rig.** The wind turbine experimental rig, as shown in Figure 2, is supplied with wind sources by a small wind tunnel. In order to create experimental conditions with different wind speeds, a 15kW axial flow fan was installed, which was controlled by a variable frequency drive. This experiment rig consists of wind wheel, The primary shaft bearings and generator utilize spherical roller bearings, which are primarily designed to support radial loads. Additionally, these bearings can handle some axial loads, typically induced by the wind's impact on the turbine blades. The wind wheel shaft and generator is connected by a coupling. Generator output terminal is connected with storage battery through an AC-DC converter. A wind sensor is employed to gauge the velocity of the wind, while a photoelectric switch sensor is utilized to determine the rotational speed of the wind turbine. An acceleration sensor is installed on bearing pedestal to collect bearing's vibration acceleration signal. The experimental sampling frequency is 2kHz.

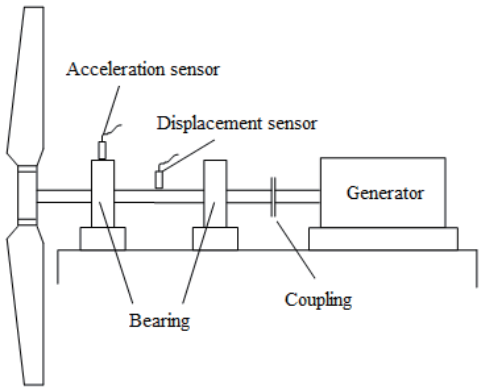

FIGURE 2. Test stand of direct-drive wind turbine.

To investigate potential localized damage in spherical roller bearings, which can affect the outer ring, inner ring, and rollers, a series of experiments was conducted using four 22206-type spherical roller bearings. These bearings have an outer diameter of 62 mm, an inner diameter of 30 mm, and a thickness of 20 mm. One bearing is kept in its original, undamaged state, while the other three are intentionally damaged to simulate different fault conditions: an inner ring defect, an outer ring defect, and a roller defect. The defects are created by cutting slots into the respective components using a wire cutting technique. These slots' width is 0.2mm, depth is 0.3mm. The fault bearing is installed on close to the wind turbine side.

4.2. **Results and analysis.** The experimental frequency of the wind turbine is set at 4.17 Hz. At this frequency, the vibration acceleration signals for bearings with defects in the inner race, outer race, and rollers are illustrated in Figure 3. Additionally, the figure presents the initial four PRCs (c_i) obtained by decomposing the vibration acceleration signals using the ITD technique. The analysis reveals that in four states the first PRC c_1 contains the original signals' main information. The c_1 has obvious fault shock characteristics. The instantaneous amplitude and instantaneous phase of c_1 in four states are extracted. They are analyzed in frequency spectrum as shown in Figure 4. In order to observe easily the instantaneous phase, this figure only gives the phase diagram in the 0∼0.1s. Instantaneous amplitude and instantaneous phase directly reflects the characteristics of the vibration signal, so in this paper the instantaneous amplitude feature and instantaneous phase feature of c_1 in four states are extracted. These features can effectively represent the original signal's state characteristics. That the selected feature vectors are: $AP_1 = [A_1(u_{mf}), A_1(u_{fc}), A_1(u_{rmsf}), A_1(u_{stdf}), P_1(u_{mf}), P_1(u_{fc}), P_1(u_{rmsf}), P_1(u_{stdf})]$, where $A_1(u_{mf}), A_1(u_{fc}), A_1(u_{rmsf})$ and $A_1(u_{stdf})$, denote respectively the mean frequency, frequency center, frequency root mean square value and frequency standard deviation value of the first proper rotation component's instantaneous amplitude; $P_1(u_{mf}), P_1(u_{fc}), P_1(u_{rmsf})$ and $P_1(u_{stdf})$ denotes respectively the mean frequency, frequency center, frequency root mean square value and frequency standard deviation value of the first proper rotation component's instantaneous phase. Through

analysis, it was discovered that the first inherent rotational component c_1 encompasses the main information of the original signal and has obvious fault impact characteristics. Its instantaneous amplitude spectrum was analyzed. It can be perceived that in the instantaneous amplitude spectrum map of the c_1 component of the outer ring fault, there is a clear spectral line at the fault characteristic frequency of 23.44 Hz in the outer ring fault of the bearing, which is close to the calculated frequency, indicating that the self-aligning roller bearing has an outer ring fault.In the instantaneous amplitude spectrum chart of c_1 inner ring fault, the characteristic frequency of inner ring fault of the bearing, 33.2 Hz, can be clearly seen, which is close to the theoretical calculated frequency, indicating that the spherical roller bearing has inner ring fault. In the instantaneous amplitude spectrum chart of c_1 rolling body fault, the distinct frequency of the bearing's roller defect, 11.73 Hz, is evident and closely matches the theoretically predicted frequency, confirming the presence of a roller fault in the spherical roller bearing.

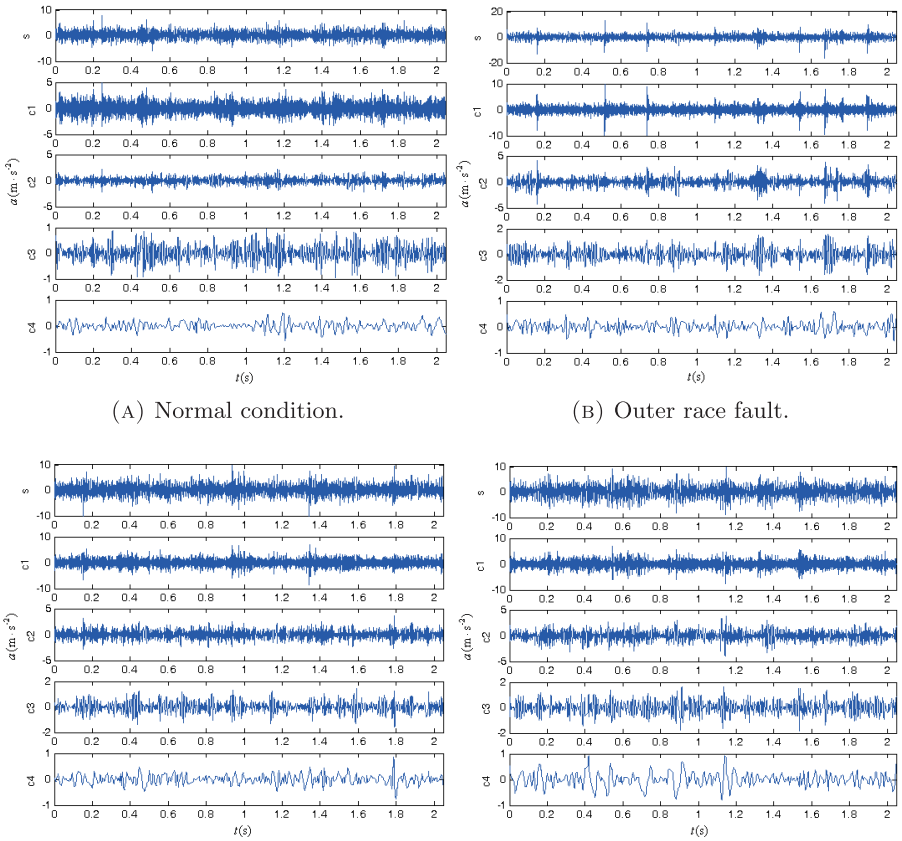

(A) Normal condition. (B) Outer race fault.

(C) Inner race fault. (D) Roller fault.

FIGURE 3. Vibration acceleration signals and their former four proper rotation components of direct-drive wind turbine in different conditions.

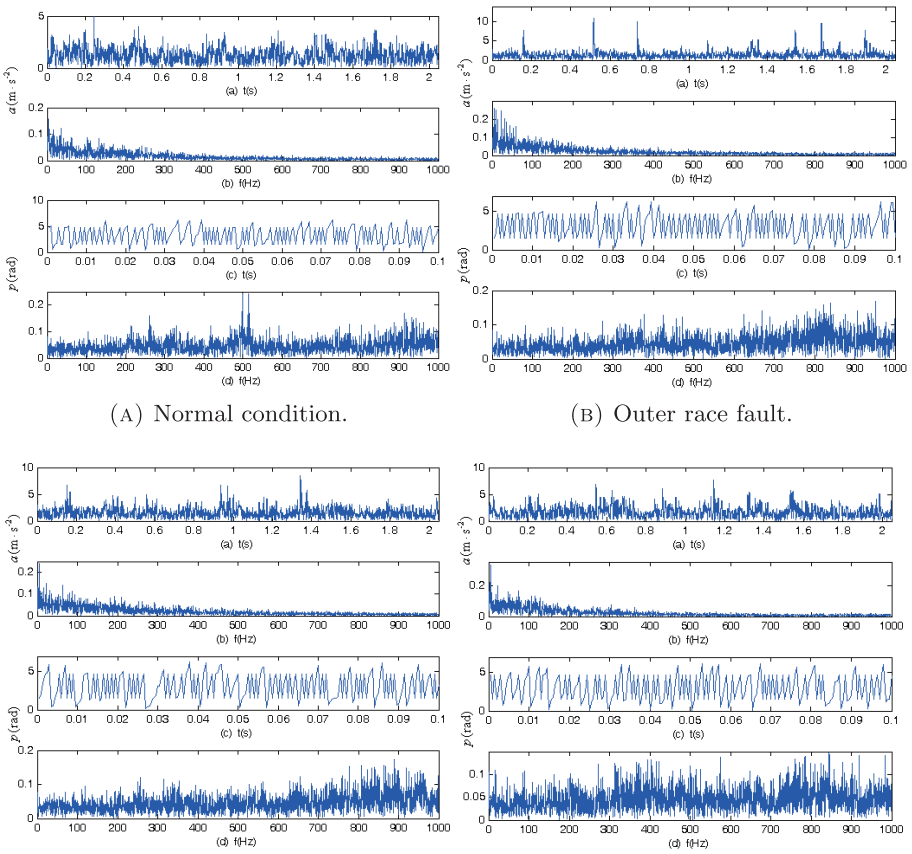

(A) Normal condition. (B) Outer race fault.

(C) Inner race fault. (D) Roller fault.

FIGURE 4. The immediate magnitude, the instantaneous angle, and their corresponding spectral characteristics of the primary inherent rotational elements within vibration acceleration data under various scenarios.

Vibration acceleration data from wind turbine bearings are gathered across four distinct conditions: normal operation, outer race defect, inner race defect, and roller defect. For each condition, 30 datasets are collected, resulting in a total of 120 datasets. Table 1 presents 32 feature vectors for these four conditions, derived from the spectral analysis of the instantaneous amplitude and frequency of the primary rotational component. Where $A_1(u_{mf}), A_1(u_{fc}), A_1(u_{rmsf}), A_1(u_{stdf})$, represents respectively the mean frequency, frequency center, frequency root mean square value and frequency standard deviation value of the first proper rotation component's instantaneous amplitude. The $P_1(u_{mf}), P_1(u_{fc}), P_1(u_{rmsf}), P_1(u_{stdf})$, denotes respectively the mean frequency, the central frequency, the root mean square frequency, and the standard deviation of the frequency for the instantaneous phase of the primary proper rotational component.

As can be seen from Table 1, the difference between fault signals and normal signals is more clearly manifested in the instantaneous phase feature. The difference

between Roller fault and the normal state is the smallest in all components, while the differences between the other two faults and the normal state are more obvious. The difference between Outer race fault and Inner race fault in a single component is small, but when viewed as a whole, there is still a difference that can be further identified by a neural network.

TABLE 1. Spherical roller bearing fault feature of direct-drive wind turbine based on instantaneous amplitude and instantaneous phase of ITD.

No.	Bearing state	Instantaneous amplitude features				Instantaneous phase features			
		$A_1(u_{mf})$	$A_1(u_{fc})$	$A_1(u_{rmsf})$	$A_1(u_{stdf})$	$P_1(u_{mf})$	$P_1(u_{fc})$	$P_1(u_{rmsf})$	$P_1(u_{stdf})$
1	Normal condition	46.37	259.02	368.41	261.98	100.62	493.06	576.18	298.11
2		44.95	256.87	368.38	264.05	101.04	493.39	575.51	296.27
3		44.99	256.38	366.87	262.41	101.02	497.84	579.99	297.57
4		44.47	261.61	371.77	264.15	101.44	493.27	575.7	296.84
5		45.42	265.63	375.59	265.51	101.02	495.53	576.72	295.05
6		43.42	259.96	369.98	263.27	100.75	490.71	571.76	293.45
7		40.76	263.5	372.4	263.15	100.59	493.23	575.3	296.14
8		42.8	260.45	371.23	264.53	101.52	493.33	575.85	297.02
9	Outer race fault	44.46	274.94	379.75	261.94	98.32	529.38	614.54	312.1
10		43.52	273.79	378.37	261.15	97.27	532.58	617	311.53
11		44.02	280.05	385.61	265.08	97.51	530.48	614.74	310.64
12		45.36	274.49	378.92	261.22	96.27	531.99	617.23	312.99
13		42.9	274.06	378.61	261.21	97.14	530.33	614.94	311.28
14		43.11	276.8	380.89	261.64	97.76	530.05	614.96	311.81
15		42.84	277.32	381.24	261.6	96.92	531.58	615.94	311.14
16		44.75	274.91	380.21	262.65	97.94	528.44	613.54	311.73
17	Inner race fault	47.52	260.65	371.86	265.2	99.08	520.27	602.66	304.15
18		46.08	269.04	376.73	263.69	99.16	520.66	603.96	306.06
19		44.98	269.57	378.72	266.01	98.67	519.62	603.12	306.19
20		45.29	267.53	373.71	260.93	98.86	522.92	605.32	304.91
21		56.77	251.09	362.98	262.12	99.64	512.54	595.92	304
22		49.81	260.46	368.99	261.37	99	520.26	604.03	306.89
23		50.32	256.66	366.85	262.12	98.26	524.27	607.08	306.08
24		50.28	263.88	371.07	260.87	98.59	522.15	604.88	305.33
25	Roller fault	31.77	271.57	379.65	265.3	99.07	501.38	586.5	304.3
26		33.77	266.74	374.1	262.29	99.16	503.79	589.44	306
27		32.31	268.4	377.22	265.06	99.25	499.28	583.18	301.35
28		33.34	274.16	380.7	264.14	98.05	504.09	589.1	304.85
29		32.07	273.86	380.5	264.15	99.37	503.66	588.23	303.88
30		33.45	270.12	377.42	263.58	99.64	502.53	586.88	303.14
31		33.32	271.79	378.93	264.04	99.14	503.4	588.18	304.22
32		34.47	271.68	379.22	264.57	99.24	500.88	586.37	304.87

In the 120 sets vibration acceleration data for four states of wind turbine bearings, 60 sets (15 sets of each state) are randomly selected as standard sample inputting neural network to train, the remaining 60 data sets are utilized as test samples for validation. The test outcomes show that all the test samples are correctly recognized. The neural elements of the input layer of neural network takes 8 (instantaneous amplitude features and instantaneous phase features), The output layer consists of 4 neurons, each representing a distinct state of the wind turbine's main bearing. The hidden layer is composed of 10 neural units. The network's performance target is a root mean square error below 1e-8 between the actual and expected outputs. Testing revealed that the trained neural network model achieved perfect accuracy in diagnosing bearing faults, with good performance.

To assess the computational effectiveness of the ITD method, it was utilized to analyze vibration signals from a wind turbine under various conditions: outer ring defect, inner ring defect, rolling element defect, and no defect. This was contrasted with the EMD method, a prevalent technique for analyzing non-stationary signals that is also effective in extracting fault features from wind turbine bearings. The findings are detailed in Table 2. According to the data, the ITD method demonstrates superior decomposition efficiency and is well-suited for the analysis of real-time, non-stationary signals, making it suitable for online fault diagnosis.

TABLE 2. Comparison of signal decomposition efficiency of ITD and EMD

	Outer race fault	Inner race fault	Roller fault	Roller fault
ITD	0.110s	0.125s	0.093s	0.047s
EMD	2.093s	1.610s	1.562s	1.094s

5. Conclusions

ITD method is capable of decomposing complex, unsteady and nonlinear vibration signal into several PRCs. The instantaneous amplitude and instantaneous phase containing obvious periodic impulse components is analyzed based on the frequency spectrum. This can effectively Measure the characteristic value of the complex signal,. Thus, despite the wind turbine bearing fault signal being nontationary and nonlinear, wind turbine diagnosis based on ITD instantaneous information can be accomplished well. The findings suggest that the ITD technique is highly effective for identifying faults in wind turbine bearings, while also offering impressive computational speed.

The fault label information in the text is still limited, and more fault labels will be added in the future to couple with the data information to improve the effectiveness of feature representation.

References

[1] X. An and D. Jiang, *Bearing fault diagnosis of wind turbine based on intrinsic time-scale decomposition frequency spectrum*, Proc IMechE, Part O: Journal of Risk and Reliability **228** (2014), 558–566.

[2] X. An, D. Jiang and S. Li, *Application of the ensemble empirical mode decomposition and Hilbert transform to pedestal looseness study of direct-drive wind turbine*, Energy **36** (2011), 5508–5520.

[3] X. An, L. Pan and L. Yang, *Condition parameter degradation assessment and prediction for hydropower units using Shepard surface and ITD*, Transactions of the Institute of Measurement and Control **36** (2014), 1074–1082.

[4] X. An, H. Zeng and C. Li, *Demodulation analysis based on adaptive local iterative filtering for bearing fault diagnosis*, Measurement **94** (2016), 554–560.

[5] X. An, H. Zeng and W. Yang, *Fault diagnosis of a wind turbine rolling bearing using adaptive local iterative filtering and singular value decomposition*, Transactions of the Institute of Measurement and Control,**39** (2017), 1643–1648.

[6] P. Esvan-Jesús, P. Vicenc and L. Francisco-Ronay, *Robust fault diagnosis of wind turbines based on MANFIS and zonotopic observers*, Expert Systems with Applications **235** (2024): 121095.

[7] *Global Wind Report 2024*, Global Wind Energy Council, 2024.
[8] J. Guo, Y. Liu and R. Yang, *Ensemble difference mode decomposition based on transmission path elimination technology for rotating machinery fault diagnosis*, Mechanical Systems and Signal Processing **212** (2024): 111330.
[9] Y. Lei, Z. He and Y. Zi, *Fault diagnosis based on novel hybrid intelligent model*, Chinese Journal of Mechanical Engineering **44** (2008), 112–117.
[10] Z. Wang, X. Yang and J. Huang, *Fault diagnosis of turnout switch machine based on ITD-SDP image features and DSCNN*, Journal of Railway Science and Technology **45** (2023), 65–71.
[11] T. Wang and L. Yin, *Dual-module multi-head spatiotemporal joint network with SACGA for wind turbines fault detection*, Energy **308** (2024), 132906–132906.
[12] J. Yu, J, Lü and H. Cheng Hui, *Rolling bearing fault diagnosis based on ITD and improved morphological filtering*, Journal of Beijing University of Aeronautics and Astronautics **44** (2018), 241–249.

Manuscript received October 12, 2024
revised December 15, 2024

X. An
China Institute of Water Resources and Hydropower Research, Haidian District, Beijing 100038, China
E-mail address: lory2366@163.com

T. Wu
China Institute of Water Resources and Hydropower Research, Haidian District, Beijing 100038, China
E-mail address: wtt2020@163.com

Z. Fu
China Institute of Water Resources and Hydropower Research, Haidian District, Beijing 100038, China
E-mail address: fzhappy356@163.com

Y. Lu
China Institute of Water Resources and Hydropower Research, Haidian District, Beijing 100038, China
E-mail address: lyingyu39021@126.com